# Laser Stimulation of Auditory Neurons: Effect of Shorter Pulse Duration and Penetration Depth

Agnella D. Izzo,*† Joseph T. Walsh Jr.,† Heather Ralph,‡ Jim Webb,‡ Mark Bendett,‡ Jonathon Wells,‡ and Claus-Peter Richter*†§

*Department of Otolaryngology, Northwestern University, Chicago, Illinois 60611; †Department of Biomedical Engineering, Northwestern University, Evanston, Illinois 60208; ‡Aculight Corp., Bothell, Washington 98021; and §Auditory Physiology Laboratory (The Hugh Knowles Center), Department of Communication Sciences and Disorders, Northwestern University, Evanston, Illinois 60208

ABSTRACT We have pioneered what we believe is a novel method of stimulating cochlear neurons, using pulsed infrared radiation, based on the hypothesis that optical radiation can provide more spatially selective stimulation of the cochlea than electric current. Very little of the available optical parameter space has been used for optical stimulation of neurons. Here, we use a pulsed diode laser (1.94 $\mu$m) to stimulate auditory neurons of the gerbil. Radiant exposures measured at CAP threshold are similar for pulse durations of 5, 10, 30, and 100 $\mu$s, but greater for 300-$\mu$s-long pulses. There is evidence that water absorption of optical radiation is a significant factor in optical stimulation. Heat-transfer-based analysis of the data indicates that potential structures involved in optical stimulation of cochlear neurons have a dimension on the order of $\sim$10 $\mu$m. The implications of these data could direct further research and design of an optical cochlear implant.

## INTRODUCTION

Pulsed midinfrared lasers have been used to evoke neural activity in motor systems and sensory systems as an alternative to electrical stimulation (1–3). The use of lasers to evoke neural responses has several appealing features as compared to electrical stimulation: no direct contact is necessary between the stimulating source and the tissue, spatial resolution of stimulation can be improved, and no stimulation artifact is generated hindering simultaneous recordings of electrical responses from the neurons. However, only a small portion of the available optical parameter space has been investigated in the optical stimulation of nerves (4,5). In addition, parameters that are optimized for one application, such as motor nerve stimulation, are not necessarily the ideal parameters to be used for stimulation of a sensory system, such as the cochlea. In fact, appropriate laser parameters, such as wavelength that dictates light distribution, are highly dependent on tissue morphology.

The use of optical stimulation in the auditory system could be beneficial for cochlear implants. In the mammalian cochlea, high frequency tones activate spiral ganglion neurons in the base of the cochlea, and low frequency tones activate neurons in the apex; a distribution known as tonotopicity (6–11). In individuals who are profoundly hearing impaired, multiple-electrode cochlear implants are designed to stimulate electrically discrete spiral ganglion cell populations along the cochlea to restore the tonotopic responses of the normal acoustically stimulated cochlea. A successful multichannel cochlear implant should, therefore, transfer a maximum of information to discrete, spatially selected groups of auditory neurons. Stimulation by one electrode should not affect the neural response to stimulation resulting from neighboring electrodes.

The assumption that discrete neural populations can be activated electrically is, however, not always true. Although it is widely assumed that stimuli applied between closely spaced bipolar electrodes can stimulate spiral ganglion cells locally (12,13), it has been shown that closely spaced electrode pairs will activate a broad region of auditory neurons at high current levels (12,14). In addition, psychoacoustic experiments (15–18) and electrophysiological studies (12,19–21) showed that current injected into the cochlea spreads via the scala tympani and, consequently, stimulates large populations of spiral ganglion cells. If two electrodes stimulate the same neural population, sound sensation encoded via these two electrode contacts might be confused or even be indistinguishable. The electrode interaction reduces the number of independent channels, and thus frequency bands, that can be used by a cochlear implant user to parallel process acoustic information. Recently, however, the interaction of electrical fields has been used to generate more pitch percepts between two electrodes (current steering) (22,23). Here, it is not the amount of information that is reduced but rather the rate by which information is transferred.

The limitation of spatial selectivity is based on fundamental physical principles of electrical stimulation that even the best electrode design has not yet overcome. By substituting optical sources for electrodes in cochlear implants, it may be possible to confine neural activation to spiral ganglion cells immediately adjacent to the stimulating optical source. Spatial confinement of neural activation could lead to improved performance by implant users. We have shown that optical stimulation of gerbil cochleae is more selective than electric stimulation ((24), A. D. Izzo, A. Lin, P. Littlefield, J. T. Walsh Jr., M. Oberoi, and C.-P. Richter, unpublished).

*Submitted July 11, 2007, and accepted for publication October 31, 2007.*

Address reprint requests to Agnella D. Izzo, Tel.: 312-503-4027; E-mail: a-izzo@northwestern.edu.

Editor: Ian Parker.



0006-3495/08/04/3159/08 $2.00

doi: 10.1529/biophysj.107.117150

Here, we present data using a different stimulating wavelength, 1.94 $\mu$m, and use shorter stimulating pulses, down to 5 $\mu$s, than in previous studies to stimulate the auditory system of the gerbil. Previously, we presented evidence that optical pulses as short as 35 $\mu$s could induce laser stimulation of the auditory system (4). In addition, stimulating with a different wavelength gives further confirmation that water absorption plays a significant role in optical nerve stimulation (4). We have hypothesized that the primary light-tissue interaction that governs optical nerve stimulation is light absorption by water in the tissue (2,3,26).

## MATERIALS AND METHODS

All measurements were made in vivo using adult gerbils (*Meriones unguiculatus*). The care and use of the animals in this study were carried out in accordance with the National Institutes of Health Guide for the Care and Use of Laboratory Animals and was approved by the Animal Care and Use Committee of Northwestern University.

### Animal surgery and preparation

Animal surgery was conducted as described previously (27). In brief, gerbils were anesthetized by an initial intraperitoneal injection of sodium pentobarbital (80 mg/kg body weight). Maintenance doses were 17 mg/kg body weight and were given throughout an experiment whenever the animal showed signs of increasing arousal, which was assessed every 30 min by a paw withdrawal reflex. After the animal was fully anesthetized, breathing was facilitated by performing a tracheotomy and securing a length of PE90 tubing into the opening in the trachea. The animal was then positioned, belly up, on a heating pad used to maintain body temperature at 38°C, and its head was stabilized in a heated head holder. A dermal incision was made from the lower right jaw to the right shoulder to expose the right submandibular gland, which was subsequently ligated and removed. The muscles attached to the bulla and to the styloid bone were carefully dissected. Next, the bulla was opened to allow access to the cochlea. A silver electrode was hooked onto the bony rim of the round window of the cochlea, and a ground electrode was placed under the skin at the left jaw. After cutting the cartilaginous outer ear canal, a speculum (to connect the sound delivery system) was cemented with dental acrylic to the bony part of the outer ear canal. The surgical platform containing the animal was then moved onto a vibration isolation table in a soundproof booth. Two chest electrodes were attached to monitor heart rate. For acoustic stimulation, a headphone (DT770Pro, Beyer, Heilbronn, Germany) was coupled to the speculum at the ear canal.

### Acoustic measurements

#### *Sound stimuli*

Voltage commands for the stimuli were generated using a computer I/O board (KPCI 3110, Keithley, Cleveland, OH) inserted into a personal computer and were used to drive a headphone (DT770Pro, Beyer). For compound action potential (CAP) measurements, tone bursts (12 ms duration, including a 1 ms rise/fall) with different carrier frequencies were presented at a rate of 4 Hz. The speculum of the speaker was coupled with a short plastic tubing to the ear canal. Sound pressure was calibrated with a real head coupler using an 1/8 inch Bruel & Kjaer microphone.

#### *Compound action potential recordings*

CAPs were measured using a modified tracking procedure (28,29). The computer I/O board (Kiethley) was used to acquire the waveforms at a 250 kHz sampling rate. CAPs were measured between 50 kHz and 2 kHz, with a resolution of 6 steps/octave. CAP threshold was defined as 30 $\pm$ 3 $\mu$V (N1/P1 amplitude). Thirty-two waveforms, presented in opposite phase, were averaged for a single measurement.

### Optical stimulation

A diode laser (Capella RINS, Aculight, Bothell, WA) was used for the optical stimulation of the auditory nerves. The laser emits infrared radiation approximately between 1.92 and 1.94 $\mu$m, by varying the temperature of the diode. Pulse durations were selected between 5 and 300 $\mu$s and the repetition rate of the laser was 2 Hz. The laser output was coupled to a low-OH 200-$\mu$m-diameter optical fiber (FIP series, Polymicro, Phoenix, AZ). The distal end of the fiber was heated and maintained to 36°C with a heating wire coil (NI60, Omega, Stamford, CT) to prevent hearing loss upon cooling of the cochlea.

The optical fiber was mounted on an x-y-z translator (Narishge, MMW-203, East Meadow, NY) attached to a micromanipulator to control the fine position. The optical fiber was inserted at the basal turn of the cochlea, approximated to the round window membrane without penetrating it, and oriented toward the modiolus (Fig. 1). The fiber was fixed in place, as close as possible toward the modiolus. It is important to note that the distal end of the optical fiber was inserted past the recording electrode and did not irradiate the measuring electrode. Radiant exposures, as measured at the distal tip of the fiber, ranged from 0.05 to 50 mJ/cm$^2$. All laser parameters (radiant exposure, pulse duration, repetition rate, and wavelength) were known and continuously monitored through a user interface.

Optically evoked CAPs were recorded using a silver electrode at the round window. Responses to 10 stimulus presentations were averaged for each measurement. The CAP threshold for optical stimulation (30 $\mu$V CAP, N1 minimum to P1 maximum) was determined at pulse durations of 5, 10, 30, 100, and 300 $\mu$s, at 1.937 $\mu$m. In another set of experiments, the wavelength was varied between 1.923 and 1.937 $\mu$m and the CAPs were recorded while the pulse duration was held at 30 $\mu$s.

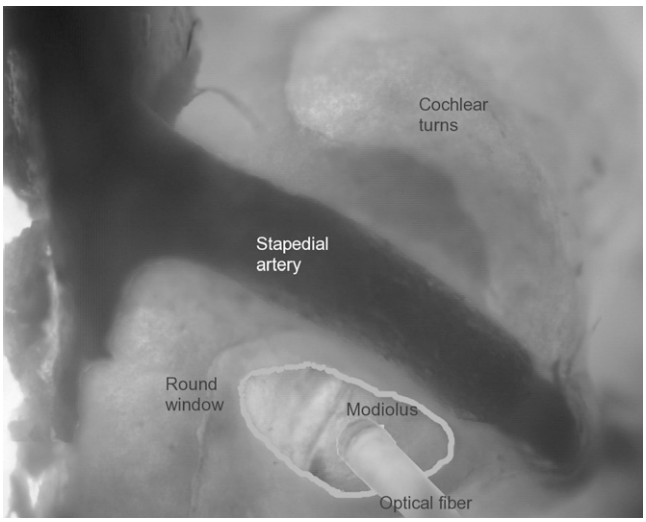


FIGURE 1 Optical fiber insertion into the cochlea. This image of the experimental setup indicates the surgical access to the gerbil cochlea and the insertion of the optical fiber. The optical fiber is placed at the round window opening and is directed toward the modiolus, the central supporting structure of the cochlea that houses the projections of the spiral ganglion cells toward the central nervous system. The round window and the stapedial artery are shown as reference points. This image was compiled from serial photos of different focal planes of the cochlea.

### Data analysis

Mean, standard deviation, and standard error were calculated for the data obtained when the pulse duration was varied. To determine whether differences between averages were significant, a one-way analysis-of-variance (ANOVA) was done for each set of measurement. If significant overall changes were found, pairwise comparisons were made using a Tukey-honestly-significant-difference test with a 5% significance criterion.

## RESULTS

A total of 14 animals were used in the experiments. All animals had normal acoustic thresholds, which were not affected by laser radiation. Attempts to optically evoke CAPs using the previous placement and orientation of the optical fiber (4) were not successful. Therefore, the optical fiber was directed at the modiolus (containing the central projections of the spiral ganglions cells) in the basal turn of the cochlea. In this orientation, CAPs were evoked in response to optical pulses as short as 5 $\mu$s (Fig. 2). The CAPs for the shorter duration pulses were composed primarily of one negative peak (N1) followed by one positive peak (P1). For the longest duration optical pulses, 300 $\mu$s, the electrical responses from the cochlea became more complex: the area under the curve of P1 broadened as compared to shorter pulse durations. Evoked responses for increasing radiant exposures (input-output (I/O) curves) were recorded for all optical pulse durations for each animal (Fig. 3). At the shortest pulse duration of 5 $\mu$s, the CAP amplitude increased monotonically as the radiant exposure was increased to the maximum available from the laser source (Fig. 3 *a*). For 30-$\mu$s-long pulses, the I/O curve showed a monotonic increase in CAP amplitude with increasing radiant exposure, followed by a plateau in CAP amplitude for radiant exposures $>\sim$15 mJ/cm$^2$ (Fig. 3 *b*). This trend was seen for each animal, independent from the absolute CAP amplitude values. I/O curves for 100- and 300-$\mu$s-long pulses (data not shown) exhibited trends similar to the ones shown for 30-$\mu$s-long pulses: a monotonic increase in CAP amplitude in response to radiant exposures of 21 and 61 mJ/cm$^2$, respectively, followed by an apparent plateau.

The threshold for the optically evoked response (CAP amplitude for N1 to P1 of 30 $\mu$V) was measured for each pulse duration (Fig. 4). The threshold radiant exposures were as follows (mean $\pm$ SE, $n = 11$): 5 $\mu$s: 1.6 $\pm$ 0.2 mJ/cm$^2$; 10 $\mu$s: 2.1 $\pm$ 0.3 mJ/cm$^2$; 30 $\mu$s: 2.9 $\pm$ 0.6 mJ/cm$^2$; 100 $\mu$s: 4.1 $\pm$ 0.4 mJ/cm$^2$; 300 $\mu$s: 15.1 $\pm$ 2.2 mJ/cm$^2$. When the

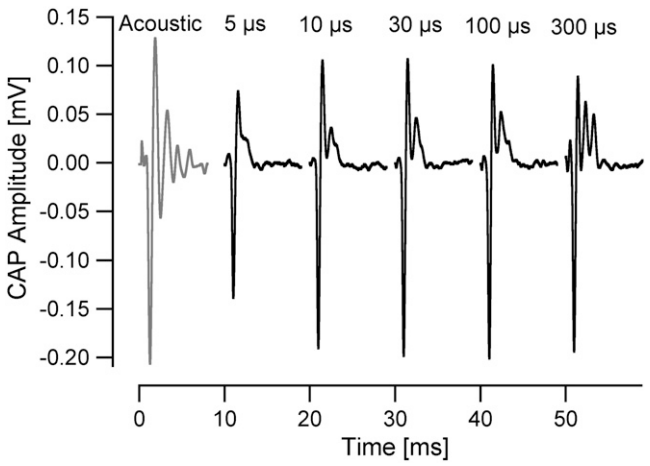


FIGURE 2 CAPs evoked from the gerbil cochlea in response to varying pulse durations. The shape of the CAPs evoked by an optical stimulus is relatively similar for a pulse 10–100 $\mu$s long. At pulse duration of 5 $\mu$s, only one positive peak is present and the maximum amplitude of the CAP is limited by the maximum output of the laser. For pulses 10–300 $\mu$s long, there is a secondary positive peak that becomes more prominent with longer pulses. These CAPs were measured from the same animal. An acoustically evoked CAP is presented on the left for comparison, elicited using one cycle of a 10 kHz tone (click) at 81 dB SPL. Each trace begins at $t = 0$, with the start of the laser pulse, and is offset in the figure for clarity.

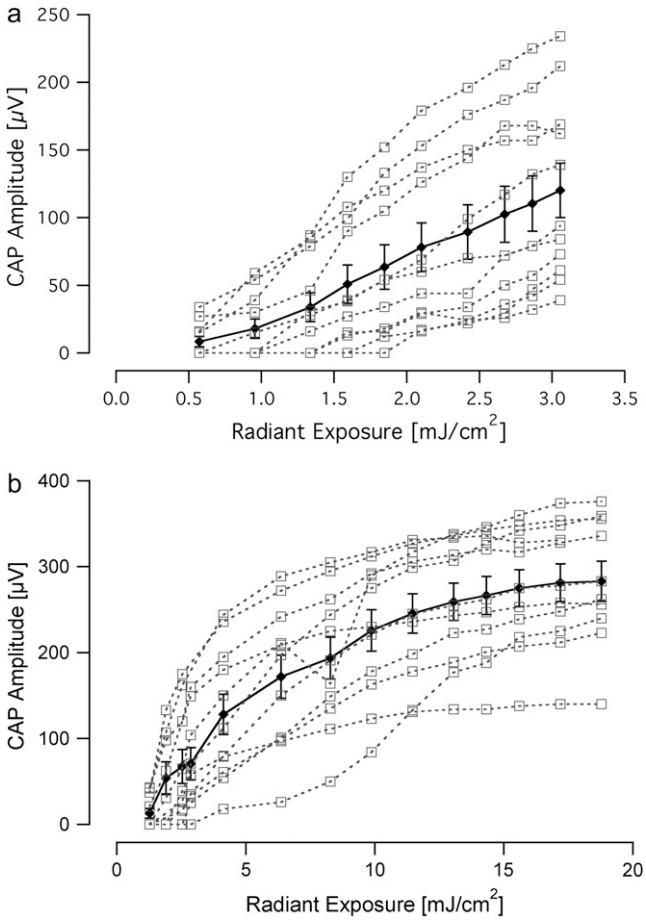


FIGURE 3 Input/output curves recorded in response to laser stimulation. (*a*) The data show the amplitude of the evoked compound action potential as the input radiant exposure is varied for a 5-$\mu$s-long optical pulse. There is a monotonic increase in evoked CAP amplitude with increasing radiant exposure. (*b*) The I/O function for a 30-$\mu$s-long pulse reveals a monotonic increase in CAP amplitude with increasing radiant exposure, followed by an apparent plateau in CAP amplitude above $\sim$15 mJ/cm$^2$. In both panels, data from individual animals ($n = 11$) are represented by open squares and the mean is shown with the standard error.

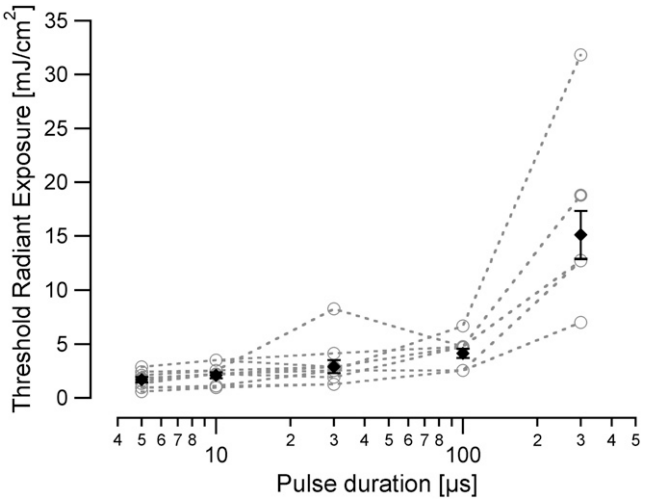


FIGURE 4 Radiant exposure needed to evoke a threshold CAP as a function of pulse duration. The radiant exposure measured at CAP threshold has a minimum value for the shortest duration pulse (5 $\mu$s); the radiant exposure increases slightly for 10-, 30-, and 100-$\mu$s-long pulses, and then increases significantly for 300-$\mu$s-long pulses. The individual data sets measured from each animal ($n = 11$) are represented by the open circles and the mean is shown with the standard error.

individual thresholds for different pulse durations were compared, differences were only significant for the 300-$\mu$s-long pulses (ANOVA, $p < 0.05$).

The I/O curves for all pulse durations measured in an individual animal revealed an interesting trend. I/O curves measured at 5, 10, and 30-$\mu$s-long pulses grouped together. In other words, the radiant exposure required to evoke a CAP of the equal magnitude was the same (Fig. 5). When the pulse duration was increased to 100 $\mu$s, there was a slight shift of the curve to higher radiant exposures to evoke the same magnitude CAP, and an even greater shift for 300-$\mu$s-long pulses.

Finally, we examined the effect of varying the wavelength of the stimulating optical radiation on the evoked response while holding the radiant exposure constant. At the shortest wavelength, 1.923 $\mu$m, we obtained the largest CAP amplitudes; increasing the wavelength to 1.937 $\mu$m, there was a slight decrease in the evoked CAP amplitude (Fig. 6). We measured a change of $-45 \pm 7$ $\mu$V (mean $\pm$ SE, $n = 10$). The evoked CAP amplitudes at 1.937 $\mu$m were significantly different than the evoked CAPs measured at 1.923 $\mu$m ($p < 0.001$).

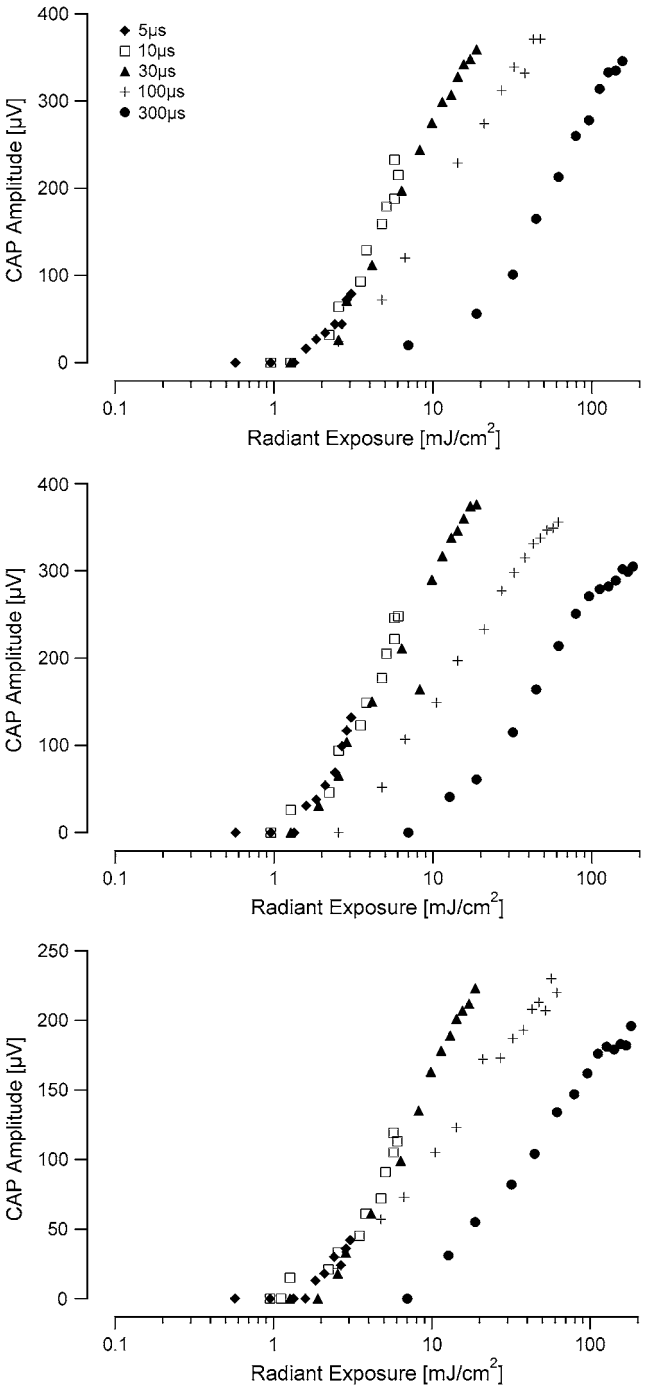


FIGURE 5 Comparison of I/O curves across pulse durations. By examining the I/O curves for each pulse duration from each animal, we find that at pulse durations of 5, 10, and 30 $\mu$s, there is a relatively similar radiant exposure needed to evoke a CAP of the same magnitude. At a pulse duration of 100 $\mu$s, a slightly higher radiant exposure is needed to evoke the same magnitude CAP, and there is a further increase in radiant exposure to evoke a CAP using a pulse duration of 300 $\mu$s. Each of the three panels shows data measured from one (different) animal. The abscissa is represented on a log scale for clarity, as opposed to Fig. 3, which represents some of the same data on a linear scale.

## DISCUSSION

We have successfully stimulated gerbil auditory neurons with optical radiation at a wavelength of $\sim$1.94 $\mu$m. Moreover, we evoked CAPs with pulses as short as 5 $\mu$s in duration. The radiant exposure required to stimulate the neurons remains relatively stable at and below 30 $\mu$s. For pulse durations of 100 $\mu$s and longer, more radiant energy is required to evoke the same neural response.

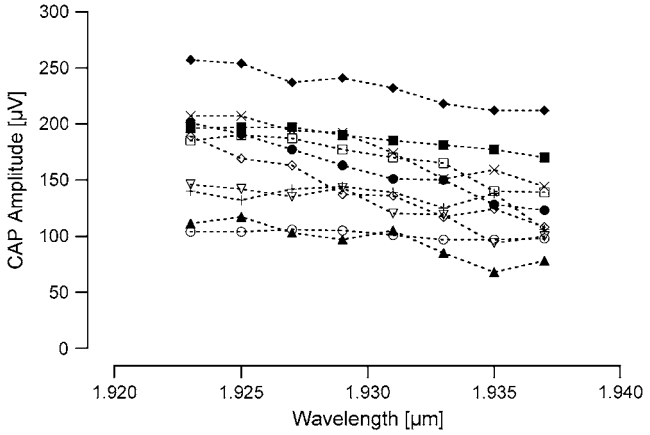


FIGURE 6 Optically evoked response as a function of changing laser wavelength. The optically evoked response increases in amplitude when the irradiating wavelength results in an increased optical penetration depth. The largest CAP amplitude is measured at 1.923 $\mu$m and the CAP amplitude is smallest at 1.937 $\mu$m. Each symbol represents data acquired from a different animal ($n = 10$).

It was necessary to modify the position of the optical fiber within the cochlea to achieve stimulation, as compared to previous experiments in which the optical fiber was directed at Rosenthal's canal, which contains the spiral ganglion cell bodies (4). The major difference between the two sets of experiments was the stimulating wavelength, $\sim$1.94 $\mu$m used for these experiments and $\sim$1.85 $\mu$m used for the previous experiments. The change of wavelength can have a significant impact on the light distribution in the tissue. We hypothesize that the major absorber of these wavelengths of light is water in the tissue. Peripheral nerve tissue is composed of $\sim$80% water, with the remainder largely composed of lipids and proteins (30,31). Examining the water absorption curve (Fig. 7) then explains the discrepancy of optical fiber position. From the known optical properties of water (32–34), we calculate that at 1.94 $\mu$m, the absorption coefficient of water is $\sim$115 $cm^{-1}$, which corresponds to an optical penetration depth of $\sim$85 $\mu$m. (Optical penetration depth is defined as the distance over which the incident light is reduced in magnitude by 1/e. At the wavelengths used in this set of experiments, the penetration depth is primarily a function of the absorption coefficient of the tissue; scattering is expected to minimally affect the penetration depth.) At 1.85 $\mu$m, the water absorption coefficient is $\sim$10 $cm^{-1}$, which gives an optical penetration depth of $\sim$1000 $\mu$m. In our previous experiments using 1.85 $\mu$m stimulating light, the distal end of the optical fiber was immersed in cochlear fluids, $\sim$500 $\mu$m away from the neurons (oriented toward the spiral ganglion cell bodies) and the energy delivered at the end of the optical fiber was reduced to $\sim$38% of the original value by the time it reached the neurons. (We use the Beer-Lambert law to calculate the axial attenuation of light: $H_z = H_0 e^{-\mu a \times z}$; where $H_0$ is the radiant exposure at distance $z = 0$ and $\mu_a$ is the absorption coefficient.) If we used a stimulating wavelength of $\sim$1.94 $\mu$m in the same experimental setup, the energy delivered at the distal tip of the optical fiber would be reduced to 0.3% of the original value by the time it reached the neurons. By simply positioning the optical fiber closer toward the modiolus, with significantly shorter distance between the optical fiber and the neurons, we circumvent the large reduction of stimulating energy by absorption of cochlear fluids.

In this set of experiments, we modified the stimulating wavelength from 1.923 to 1.937 $\mu$m, and measured a change in evoked CAP of $-45$ $\mu$V. Again, this can be explained by examining the water absorption within this wavelength range. At 1.923 $\mu$m, the optical penetration depth is $\sim$95 $\mu$m, and at 1.937 $\mu$m, the optical penetration depth is $\sim$85 $\mu$m. It is likely that, with a longer optical penetration depth at 1.923 $\mu$m, there are more auditory neurons receiving suprathreshold laser irradiation, which would contribute to a larger CAP amplitude.

Recall that the input/output curves of 5-$\mu$s, 10-$\mu$s, and 30-$\mu$s duration pulses grouped within animals, demonstrating that the same radiant exposure was required to evoke the same magnitude CAP. However, with 100-$\mu$s and 300-$\mu$s-long pulses, a larger radiant exposure was required to evoke the same magnitude CAPs. These data are consistent with the following explanation of the mechanism of action. In general, the laser energy is absorbed by the tissue and converted to heat. The data indicate that the tissue heating is spatially confined for pulses $\sim$30 $\mu$s and shorter. Energy that is deposited after $\sim$100 $\mu$s does not as significantly contribute to the generation of the CAP, i.e., the heat is no longer completely confined because some of the heat generated by the beginning of the optical pulse diffuses away from the site of absorption by the end of the pulse. A similar trend is observable in our previous data using a different stimulating wavelength: the radiant exposures needed to induce a threshold CAP increased with pulse durations longer than 35 $\mu$s (4).

The likely mechanism by which optical stimulation occurs is a small, transient increase in tissue temperature upon light absorption by water (5). A photochemical mechanism is unlikely because there is no single wavelength or narrow wavelength band at which the nerve stimulation is enhanced. In addition, the energy contained in infrared photons is too low ($<$0.1 eV) to cause a photochemical reaction. A photomechanical process has also been ruled out as a possible mechanism. Specifically, we note a lack of a cochlear microphonic in the optically evoked CAPs (3). Cochlear microphonics, which are present in acoustic CAPs, indicate deflection of cochlear hair cell cilia in response to a mechanical perturbation of the cochlear fluids. Furthermore, experiments on acute and long-term deafened gerbils indicate that it is possible to stimulate deafened cochlea in which no hair cells (the mechanoelectric transducers) exist and optically evoked CAP thresholds of deafened animals are not significantly different from normal hearing animals (deafened animals exhibit acoustic threshold elevations of $\geq$40 dB) (3,35).

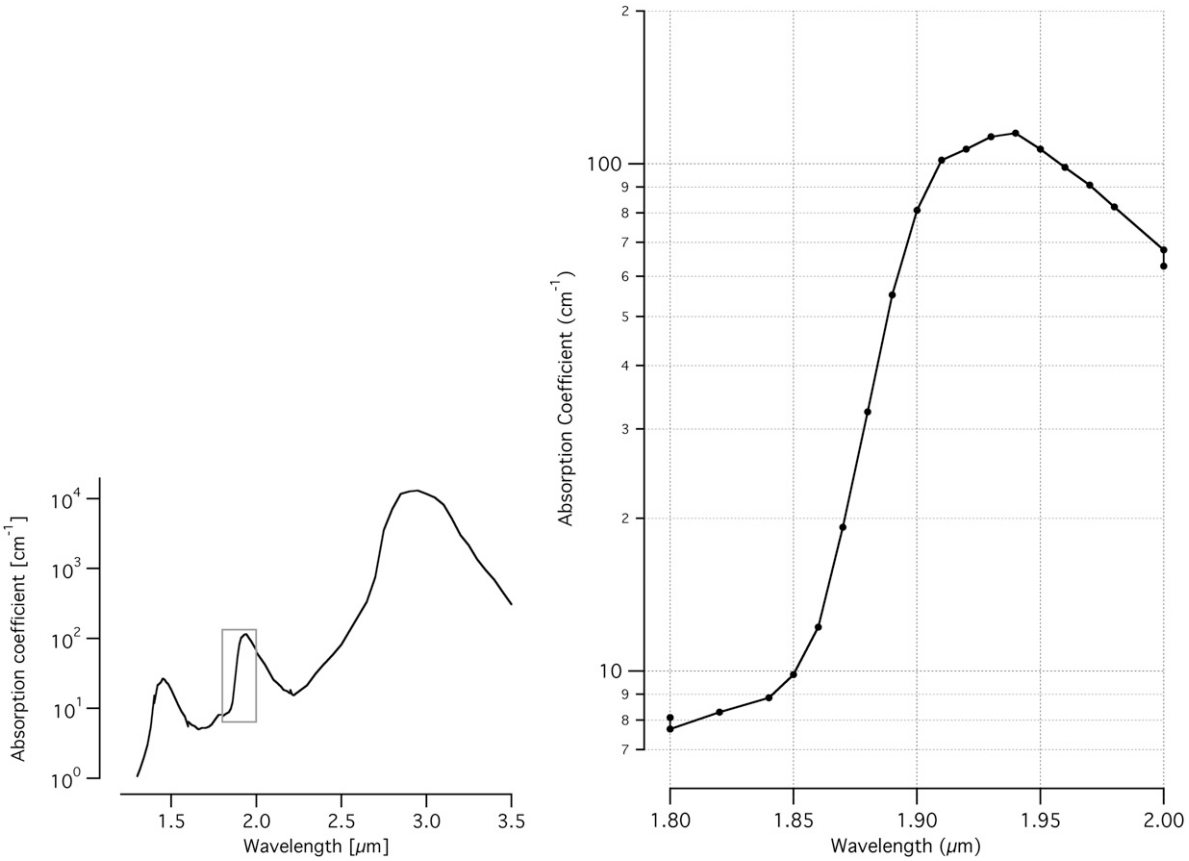


FIGURE 7 Absorption curve of water for midinfrared wavelengths. For the wavelengths used in these experiments, 1.923–1.937 $\mu$m, the water absorption coefficient is 105–115 cm$^{-1}$, which corresponds to a penetration depth of ~95–85 $\mu$m (32–34). In the previously published experiments (4), the stimulating wavelength was 1.844–1.873 $\mu$m. These wavelengths have water absorption coefficients of 9–20 cm$^{-1}$, which correspond to penetration depths of ~1120–400 $\mu$m. The shaded box indicates the region of interest that is replicated at a higher magnification on the right.

We can estimate the instantaneous temperature rise associated with cochlear nerve stimulation at time $t = 0$ after a laser pulse:

$$T(z,0) = \frac{\mu_a H(z)}{\rho c},$$

where $\mu_a$ is the wavelength-dependent absorption coefficient of the material, which would be 115 cm$^{-1}$ at 1.94 $\mu$m; *H(z)* is the radiant exposure at depth, $z$, into the tissue; $\rho$ is the density, which is 1030 kg/m$^3$ for most soft tissues; and $c$ is the specific heat of the tissue with a value of 3600 J/kg°C (36). At 1.94 $\mu$m using a radiant exposure of 5mJ/cm$^2$, the calculated temperature rise would be 0.15°C at the distal tip of the optical fiber and 0.08°C at the neurons.

It is recognized that for thermally induced laser-tissue interactions when the laser pulse is less than the thermal relaxation time of the heated target, the energy is significantly confined within the target and the process is highly efficient. In other words, laser energy is deposited and the temperature increase occurs before heat dissipates from the tissue. When the laser pulse is longer than this thermal relaxation time, energy diffuses from the target during the laser pulse, preventing the same confined temperature increase for the same laser energy deposited, and the process is less efficient (37,38). The thermal relaxation of a long cylindrical heated target can be calculated from

$$\tau_{\text{therm}} \cong \frac{x^2}{16\kappa},$$

where $\tau$ is the thermal relaxation time constant of the tissue, $x$ is the length parameter of the tissue, and $\kappa$ is the thermal diffusivity with a value of $1.4 \times 10^{-7}$ m$^2$/s (37,39). The data in Figs. 3–5 suggest that the thermal relaxation time of the target for optical stimulation is in the range of ~30–100 $\mu$s; that is, for pulses $<\sim$30 $\mu$s, the thermalized optical energy is still confined and thus a significant fraction of the optical energy contributes to the temperature rise necessary for the production of a CAP. For a thermal relaxation time of 50 $\mu$s, one calculates a length constant, $x$, of ~10 $\mu$m. Thus, it appears that the relevant tissue structure involved in the neural stimulation has a dimension on the order of a few microns. Although we cannot definitively prove the target structure with the data presented here, we note that the diameter of the central process of a spiral ganglion cell has been measured histologically to be ~3 $\mu$m (40–43).

A further comment should be made regarding the change in threshold radiant exposure with pulse duration. When one

measures an increase in the threshold radiant exposure as the pulse duration increases, two possible explanations are most obvious: 1), what matters is the temperature needed to induce a CAP, or 2), what matters is the slope of the tissue temperature versus time (i.e., the temperature rise time). We note that for pulses 5–30 $\mu$s in duration (i.e., over durations that vary by a factor of 6) there is no difference in the radiant exposure required to elicit the same amplitude CAP. Thus, for pulses 5–30 $\mu$s in duration, what matters is not the rise time but rather the temperature achieved. Further, the data indicate that if the pulse gets too long, then one needs even more energy. Thus the data indicate that the size of the target is important: that is, during a longer pulse, thermal energy diffuses away from the target during the pulse, therefore one needs more energy input during the longer pulse to overcome the thermal energy loss occurring during these longer pulses.

The time constant of 30–100 $\mu$s has important implications for a cochlear implant. An optical cochlear implant will need to deliver stimulating pulses at rates of up to 1 kHz, partly to encode information in the auditory system. Stimulating with 100-$\mu$s-long pulses at 1 kHz will allow 900 $\mu$s between pulses to allow the thermalized optical energy to dissipate. From theoretical considerations, one can estimate the necessary interpulse cooling time from the thermal relaxation time of the target. The thermal relaxation time is that time during which little thermal energy leaves the target. However, after one thermal relaxation time, significant thermal energy does not immediately leave the target. Indeed, thermal diffusion is not an exponential process. It is slower, thus it takes many thermal relaxation times for significant thermal energy to diffuse from the target (a good estimate is $\sim 10 \times \tau_{\text{therm}}$) (44–47). Consequently, if a second pulse arrives before there is significant cooling, there will be a rise in the baseline temperature of all tissue structures near the target. Using the estimated cooling time of $10 \times \tau_{\text{therm}}$, from the data presented here one calculates a maximum pulse repetition rate of ~2000 Hz, i.e., $(10 \times 50\ \mu\text{s})^{-1}$. For some laser-based medical applications, it is recommended to allow 100 thermal relaxation times to elapse for cooling before the next pulse is presented, which in our case would correspond to ~200 Hz. However, the typical applications for which these thermal relaxations times are described achieve a clinical endpoint of tissue coagulation or ablation and involve much larger temperature rises than our case. There is evidence that a pulse repetition rate faster than allowed by $100\ \tau_{\text{therm}}$ can stimulate cochlear nerves without damage. Specifically, stimulating with 35-$\mu$s-long laser pulses at 400 Hz did not show any acute damage over several hours (4). More experiments will be needed to determine the thermal relaxation of the tissue for chronic stimulation paradigms and when stimulating with multiple sources in parallel.

Given that a major objective of this research is toward constructing an optical cochlear implant, we should consider potential design issues in light of the current data. The human cochlea is a spiral structure (snail-shaped) containing fluid-filled spiral tubes, which measures ~9 mm across its base and ~5 mm from base to apex (top to bottom). The diameter of the scala tympani, in which the cochlear implant arrays are inserted, is ~2.5 mm at the base and ~1.25 mm in the middle of the cochlea. Ideally, the stimulating source would be positioned as close as possible to the neurons. The minimum distance between the scala tympani and the spiral ganglion cells, across the bony modiolar wall, is ~200 $\mu$m. The maximum distance is the wall thickness plus the scala tympani diameter. Since there would likely be a distance of 200–500 $\mu$m between the stimulating source and the neurons, it would make sense to select a stimulating wavelength(s) that give(s) optical penetration depths of 2–3 times this distance. There are several wavelengths in the midinfrared wavelength range that have such water absorption characteristics. To adequately design for variable individual anatomies and array placements, a variable wavelength source would allow for a range of penetration depths that could be programmed to the implantee and reprogrammed as the implantee was reevaluated.

From the data gathered here, we see that pulse durations from 5 to 30 $\mu$s efficiently delivered stimulating energy to the neurons. For longer pulse durations, one needs to deposit more energy to achieve the same neural stimulation. The extra energy in these longer pulses may increase the risk of an overall temperature increase of the tissue, which might become important if optical pulses are presented at a high repetition rate. Although it may seem best to use the shortest pulse duration possible, there will exist a design tradeoff with the power requirements of the laser control circuitry to generate such high optical energy in such a short time period. For the application of stimulating cochlear nerves, pulses in the range of 1–100 $\mu$s seem ideal.

This project has been funded with federal money from the National Institute on Deafness and Other Communication Disorders, National Institutes of Health, Department of Health and Human Services, under contract No. HHSN260-2006-00006-C/NIH N01-DC-6-0006.

## REFERENCES

1. Wells, J., C. Kao, E. D. Jansen, P. Konrad, and A. Mahadevan-Jansen. 2005. Application of infrared light for *in vivo* neural stimulation. *J. Biomed. Opt.* 10:064003.
2. Wells, J., C. Kao, K. Mariappan, J. Albea, E. D. Jansen, P. Konrad, and A. Mahadevan-Jansen. 2005. Optical stimulation of neural tissue *in vivo*. *Opt. Lett.* 31:235–238.
3. Izzo, A. D., C.-P. Richter, E. D. Jansen, J. Joseph, and T. Walsh. 2006. Laser stimulation of the auditory nerve. *Lasers Surg. Med.* 38:745–753.
4. Izzo, A. D., J. Joseph, T. Walsh, E. D. Jansen, M. Bendett, J. Webb, H. Ralph, and C.-P. Richter. 2007. Optical parameter variability in laser nerve stimulation: a study of pulse duration, repetition rate, and wavelength. *IEEE Trans. Biomed. Eng.* 54:1108–1114.
5. Wells, J., C. Kao, P. Konrad, T. E. Milner, J. Kim, A. Mahadevan-Jansen, and E. D. Jansen. 2007. Biophysical mechanisms of transient optical stimulation of peripheral nerve. *Biophys. J.* 93:2567–2580.
6. von Békésy, G. 1960. Experiments in Hearing. McGraw-Hill, New York.

7. Greenwood, D. D. 1990. A cochlear frequency-position function for several species–29 years later. *J. Acoust. Soc. Am.* 87:2592–2605.
8. Geier, L. L., and S. J. Norton. 1992. The effects of limiting the number of Nucleus 22 cochlear implant electrodes programmed on speech perception. *Ear Hear.* 13:340–348.
9. Friesen, L. M., R. V. Shannon, D. Baskent, and X. Wang. 2001. Speech recognition in noise as a function of the number of spectral channels: Comparison of acoustic hearing and cochlear implants. *J. Acoust. Soc. Am.* 110:1150–1163.
10. Lawson, D. 1996. Speech Processors of Auditory Prostheses. Technical Progress Report, National Institutes of Health contract 1-DC-5-2103.
11. Lawson, D., B. S. Wilson, and C. Finley. 1993. New processing strategies for multichannel cochlear prosthesis. *Prog. Brain Res.* 97: 313–321.
12. van den Honert, C., and P. H. Stypulkowski. 1987. Single fiber mapping of spatial excitation patterns in the electrically stimulated auditory nerve. *Hear. Res.* 29:195–206.
13. Busby, P. A., L. A. Whitford, P. J. Blamey, L. M. Richardson, and G. M. Clark. 1994. Pitch perception for different modes of stimulation using the Cochlear multiple-electrode prosthesis. *J. Acoust. Soc. Am.* 95:2658–2669.
14. Frijns, J. H., S. L. de Snoo, and J. H. ten Kate. 1996. Spatial selectivity in a rotationally symmetric model of the electrically stimulated cochlea. *Hear. Res.* 95:33–48.
15. Collins, M. M., M. H. Hawthorne, and K. el-Hmd. 1997. Cochlear implantation in a district general hospital: problems and complications in the first five years. *J. Laryngol. Otol.* 111:325–332.
16. Chatterjee, M., and R. V. Shannon. 1998. Forward masked excitation patterns in multielectrode electrical stimulation. *J. Acoust. Soc. Am.* 103:2565–2572.
17. Nelson, D. A., and G. S. Donaldson. 2002. Psychophysical recovery from pulse-train forward masking in electrical hearing. *J. Acoust. Soc. Am.* 112:2932–2947.
18. Throckmorton, C. S., and L. M. Collins. 2002. The effect of channel interactions on speech recognition in cochlear implant subjects: Predictions from an acoustic model. *J. Acoust. Soc. Am.* 112:285–296.
19. Black, R. C., and G. M. Clark. 1980. Differential electrical excitation of the auditory nerve. *J. Acoust. Soc. Am.* 67:868–874.
20. Spelman, F. A., B. M. Clopton, and B. E. Pfingst. 1982. Tissue impedance and current flow in the implanted ear. Implications for the cochlear prosthesis. *Ann. Otol. Rhinol. Laryngol. Suppl.* 98:3–8.
21. O'Leary, S. J., R. C. Black, and G. M. Clark. 1985. Current distributions in the cat cochlea: a modelling and electrophysiologic study. *Hear. Res.* 18:273–281.
22. Donaldson, G. S., H. A. Kreft, and L. Litvak. 2005. Place-pitch discrimination of single-versus dual-electrode stimuli by cochlear implant users. *J. Acoust. Soc. Am.* 118:623–626.
23. Koch, D. B., M. Downing, M. J. Osberger, and L. Litvak. 2007. Using current steering to increase spectral resolution in CII and HiRes 90K users. *Ear Hear.* 28:38s–41s.
24. Izzo, A. D., E. Suh, J. Pathria, D. S. Whitlon, J. T. Walsh, and C.-P. Richter. 2007. Selectivity of neural stimulation in the auditory system: a comparison of optic and electric stimuli. *J. Biomed. Opt.* 12:021008.
25. Reference deleted in proof.
26. Wells, J., C. Kao, P. Konrad, A. Mahadevan-Jansen, and E. D. Jansen. 2006. Biophysical mechanisms responsible for pulsed low-level laser excitation of neural tissue. Proc. SPIE 6084.
27. Emadi, G., C.-P. Richter, and P. Dallos. 2004. Stiffness of the gerbil basilar membrane: radial and longitudinal variations. *J. Neurophysiol.* 91:474–488.
28. Taylor, M. M., and C. D. Creelman. 1967. PEST: efficient estimates on probability functions. *J. Acoust. Soc. Am.* 41:782–787.
29. Gummer, A. W., J. W. Smolders, and R. Kline. 1987. Basilar membrane motion in the pigeon measured with the Mössbauer technique. *Hear. Res.* 29:63–92.
30. Rosenberg, H. F., and J. T. Gunner. 1959. Sodium, potassium and water contents of various components (intact, desheathed nerve, and epineurium) of fresh (untreated) medullated (sciatic) nerve of *R. ridibunda* (and some comparative data on cat sciatic). *Pflugers Arch.* 269:270–273.
31. LoPachin, R. M., and P. K. Stys. 1995. Elemental composition and water content of rat optic nerve myelinated axons and glial cells: effects of *in vitro* anoxia and reoxygenation. *J. Neurosci.* 15:6735–6746.
32. Hale, G. M., and M. R. Querry. 1973. Optical constants of water in the 200-nm to 200-$\mu$m wavelength range. *Appl. Opt.* 12:555–563.
33. Falk, M., and T. A. Ford. 1966. Infrared spectrum and structure of liquid water. *Can. J. Chem.* 44:1699–1707.
34. Walsh, J. T., and J. P. Cummings. 1994. Effect of the dynamic optical properties of water on midinfrared laser ablation. *Lasers Surg. Med.* 15:295–305.
35. Richter, C.-P., R. Bayon, A. D. Izzo, M. Otting, E. Suh, S. Goyal, J. Hotaling, and J. T. Walsh Jr. 2008. Acute and long term deafening effects on optical stimulation of auditory neurons. *Hear. Res.* In Press.
36. Duck, F. A. 1990. Physical Properties of Tissue. Academic Press, London.
37. Anderson, R. R., and J. A. Parrish. 1983. Selective photothermolysis: precise microsurgery by selective absorption of pulsed radiation. *Science.* 220:524–527.
38. Welch, A. J., and M. J. C. van Gemert, editors. 1995. Optical-Thermal Response of Laser-Irradiated Tissue. Plenum Press, New York.
39. van Gemert, M. J. C., and A. J. Welch. 1995. Approximate solutions for heat conduction: time constants. *In* Optical-Thermal Response of Laser-Irradiated Tissue. A. J. Welch, and M. J. C. van Gemert, editors. Plenum Press, New York.
40. Spoendlin, H., and A. Schrott. 1988. The spiral ganglion and the innervation of the human organ of Corti. *Acta Otolaryngol.* 105:403–410.
41. Spoendlin, H., and A. Schrott. 1989. Analysis of the human auditory nerve. *Hear. Res.* 43:25–38.
42. Ota, C. Y., and R. S. Kimura. 1980. Ultrastructural study of the human spiral ganglion. *Acta Otolaryngol.* 89:53–62.
43. Rosbe, K. W., B. J. Burgess, R. J. Glynn, and J. B. Nadol Jr. 1996. Morphologic evidence for three cell types in the human spiral ganglion. *Hear. Res.* 93:120–127.
44. Walsh, J. T., Jr., and J. P. Cummings. 1990. The effect of pulse repetition rate on the erbium laser ablation of soft and hard tissues. *In* Laser Tissue Interactions, Proc. SPIE. S. L. Jacques, editor. 12–21.
45. Jansen, E. D., R. K. Chundru, S. A. Samanani, T. A. Tibbetts, and A. J. Welch. 1993. Pulsed infrared laser irradiation of biological tissue: effect of pulse duration and repetition rate. *In* Laser-Tissue Interaction IV. S. L. Jacques, and A. Katzir, editors. 322–326.
46. Long, F. H., and T. D. Deutsch. 1987. Pulsed photothermal radiometry of human artery. *IEEE J. Quantum Electron.* 23:1821–1826.
47. Walsh, J. T., Jr. 1995. Pulsed laser angioplasty: a paradigm for tissue ablation. *In* Optical-Thermal Response of Laser-Irradiated Tissue. A. J. Welch, and M. J. C. van Gemert, editors. Plenum Press, New York.